A CLASSIFICATION OF SEVERAL YAMATO-75 CHONDRITES (V)

Yukio MATSUMOTO[1], Hideyasu KOJIMA[2] and Nobuyuki JYO[1]

[1] *Department of Mineralogical Science and Geology, Faculty of Science, Yamaguchi University, 1677-1, Yoshida, Yamaguchi 753*
[2] *National Institute of Polar Research, 9-10, Kaga 1-chome, Itabashi-ku, Tokyo 173*

Abstract: Electron microprobe studies have been made of olivines and pyroxenes in 19 Yamato-75 chondrites which were collected from the Yamato Mountains area, East Antarctica by the 16th Japanese Antarctic Research Expedition (1974–1976) (JARE-16). These chondrites are classified on the basis of textural characteristics of chondrules, matrix, plagioclase and igneous glass, and on the compositions of olivines and orthopyroxenes. As a result, the chondrites are tentatively classified as follows: type H3 (Yamato-75029), type H4 (Yamato-75096, -75269), type H4–5 (Yamato-75291), type H5–4 (Yamato-75262), type H5 (Yamato-75012, -75259), type H5–6 (Yamato-75267), type H6 (Yamato-75100, -75277, -75304), type L4 (Yamato-75019), type L4–5 (Yamato-75297), type L5 (Yamato-75017, -75270, -75288, -75289), type L6 (Yamato-75071), type LL6 (Yamato-75258).

1. Introduction

As part of the preliminary examination of Yamato meteorites collected during a period from 1975 to 1976 (MATSUMOTO, 1978), electron microprobe analyses of olivine and pyroxene in 19 chondrites have been carried out. A primary purpose of this study is to compile a catalog of the Yamato meteorites, which will be used as a guidebook in processing, allocation and distribution of the meteorites for investigators in various fields. Many of these meteorites have been preserved at low temperatures under exceptionally clean circumstances. Therefore, we had to select a method of investigation that would allow minimal contamination, even at the expense of some uncertainties of the classification.

For this purpose, thin sections were made from the near-surface portion of each meteorite. By means of an electron microprobe analyzer, the SiO_2, FeO, MgO and CaO contents of olivine and orthopyroxene in polished thin sections have been determined to obtain histograms of iron contents in the two minerals such as given by DODD *et al.* (1967). For the rapid determination of petrologic subdivision of these chondritic meteorites, VAN SCHMUS and WOOD's classification (1967) was used in this study.

2. Experimental Method

Already, the classification of 39 chondrites in the Yamato-75 meteorites was reported by one of the authors (MATSUMOTO and HAYASHI, 1980; MATSUMOTO *et al.*, 1979, 1981; MIÚRA and MATSUMOTO, 1981, 1982). The samples used in this study are 19 fragments of Yamato-75 chondrites (*i.e.* Yamato-75012,92; -75017,91; -75019,91; -75029,92; -75071,81; -75096,91; -75100,92; -75258,97; -75259,92; -75262,62; -75267,91; -75269,92; -75270,93; -75277,92; -75288,92; -75289,71; -75291,73; -75297,72; -75304,71) which originally weighed 7 to 100 g. The additional sample is Yamato-75258,97, a chondrite which weighed 971 g.

Compositional data were obtained on the carbon-coated, polished thin sections of about 25–150 mm^2 area by using JXA-50A electron microprobe and JCXA 733 superprobe microanalyzer. The instrument was operated at 15 kV and 2.0×10^{-8}A (JXA-50A), 1.3×10^{-8}A (JCXA 733) specimen current. The quantitative chemical analyses of constituent minerals were conducted with the method of BENCE and ALBEE (1968) and ALBEE and RAY (1970), by using the correction factors for 35° (JXA-50A probe) and 40° (JCXA 733) take off angle.

Measurements for each thin section were made on about 30 points in different areas of both olivine and orthopyroxene. The size of chondrules is, however, remarkably variable from section to section. So, fine-grained minerals were determined by monitoring the peak-intensities of ten elements (*i.e.* Na, K, Mg, Fe, Si, Mn, Al, Ca, Ti, Cr) with the scanning technique.

Grains with total weight percents ($SiO_2+Al_2O_3+FeO+MnO+MgO+CaO$) outside the range between 99 and 101 wt% were ascribed to inaccurate analyses and were rejected. Any analyses in which the stoichiometry was inappropriate for either olivine or orthopyroxene were also discarded. Thus, the total number of measurements was about 30 for each sample. Atomic % of magnesium, iron and calcium in olivine and orthopyroxene was calculated with the minicomputer, followed by calculation of the "percent mean deviation" proposed by DODD *et al.* (1967). In this paper, the mean deviation and "percent mean deviation" are calculated for the atomic % of iron, as in the previous works by YANAI *et al.* (1978), MATSUMOTO and HAYASHI (1980) and MATSUMOTO *et al.* (1979, 1981).

Although the parameter "percent mean deviation" has been used as an indicator of the heterogeneity of olivine and pyroxene (*cf.* DODD *et al.*, 1967), it is found that the frequency distribution of atomic % of iron is surely useful in this study.

3. Textural Characteristics

Using transmitted and reflected light, various shapes of chondrules and matrix are observed in these thin sections. The chondrules and matrix in H group chondrites are as follows: petrologic type 3 (Yamato-75029) is very sharply defined chondrules and opaque matrix (Fig. 1); petrologic types 4 and 4–5 (Yamato-75096, -75269, -75291) are well-defined chondrules and microcrystalline matrix (Fig. 2); petrologic types 5, 5–4 and 5–6 (Yamato-75012, -75259, -75262, -75267) are readily delineated chondrules and recrystallized matrix (Fig. 3); petrologic type 6 (Yamato-75100, -75277, -75304) is poorly defined chondrules and recrystallized matrix (Fig. 4). Samely, most chondrules and matrix in chondrite of L and LL groups correspond to the respective petrologic types, such as L4 (Yamato-75019) (Fig. 5), L4–5 (Yamato-75297), L5 (Yamato-75017, -75270, -75288, -75289) (Fig. 6), L6 (Yamato-75071) (Fig. 7) and LL6 (Yamato-75258) (Fig. 8).

In each thin section, some chondrules are easily defined by their shapes and others are hardly defined. Yamato-75012 shows radial and porphyritic-olivine and orthopyroxene (Fig. 9), and barred-olivine chondrules (Fig. 10); Yamato-75029, porphyritic-olivine (Fig. 11) and porphyritic-olivine and clinoenstatite (Figs. 12 and 13); 75096,

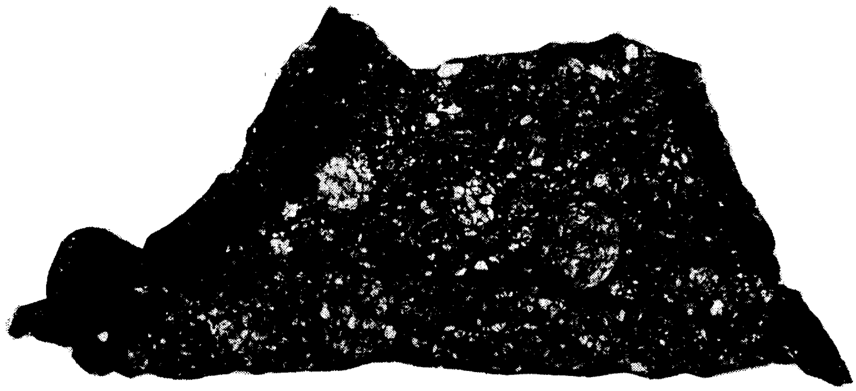

Fig . 1. Photograph of a thin section of the Yamato-75029 (type H3) chondrite showing very sharply defined chondrules and opaque matrix. Long dimension of photograph, 12 mm.

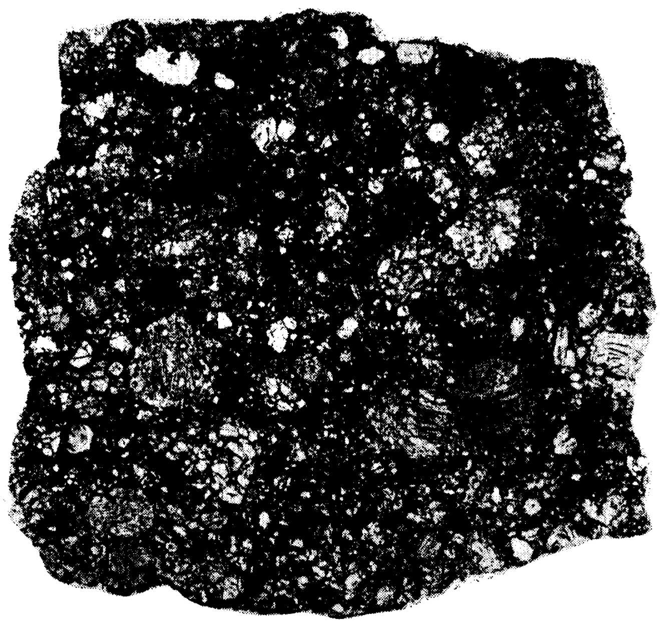

Fig. 2. Photograph of a thin section of the Yamato-75096 (type H4) chondrite showing well-defined chondrules and transparent microcrystalline matrix. Long dimension of photograph, 7 mm.

barred-olivine and radial-orthopyroxene (Fig. 14); 75100, relic porphyritic-olivine (Fig. 15); 75258, relic barred-olivine (Fig. 16); 75259, barred-olivine (Fig. 17); 75262, herringbone pattern orthopyroxene (Fig. 18); 75269, porphyritic-olivine, porphyritic-olivine and orthopyroxene, and microradiated-orthopyroxene (Fig. 19); 75270, radial-orthopyroxene and porphyritic-olivine and orthopyroxene (Fig. 20), and porphyritic-olivine (Fig. 21); 75277, radiated barred-orthopyroxene (Fig. 22); 75289, radiated barred-orthopyroxene (Fig. 23); 75291, radiated porphytitic-olivine and orthopyroxene, porphyritic-olivine, porphyritic-olivine and orthopyroxene, cryptocrystalline and radiated-orthopyroxene (Figs. 24, 25 and 26) chondrules. Cryptocrystalline and microcrystalline textures are also preserved (Figs. 19 and 26). Some chondrules show

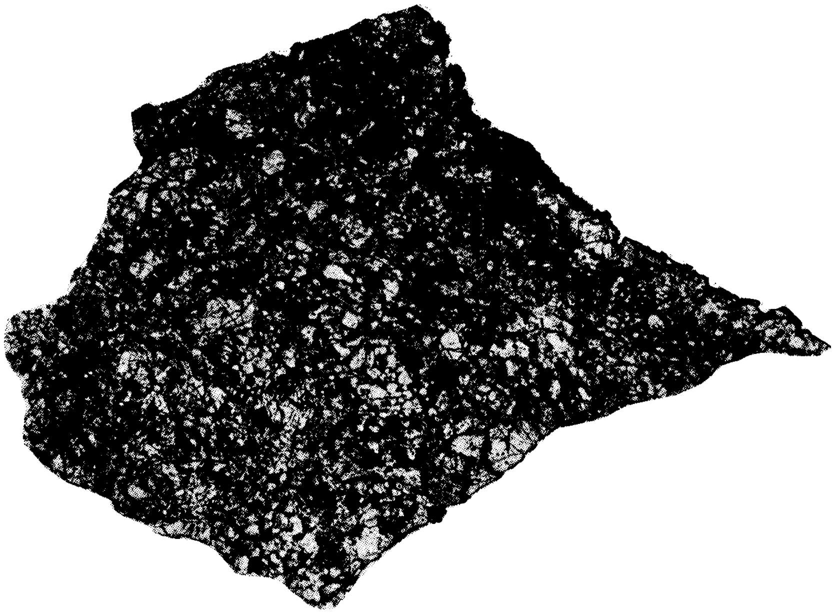

Fig. 3. Photograph of a thin section of the Yemato-75259 (type H5) chondrite showing readily delinated chondrules and recrystallized matrix. Long dimension of photograph, 8 mm.

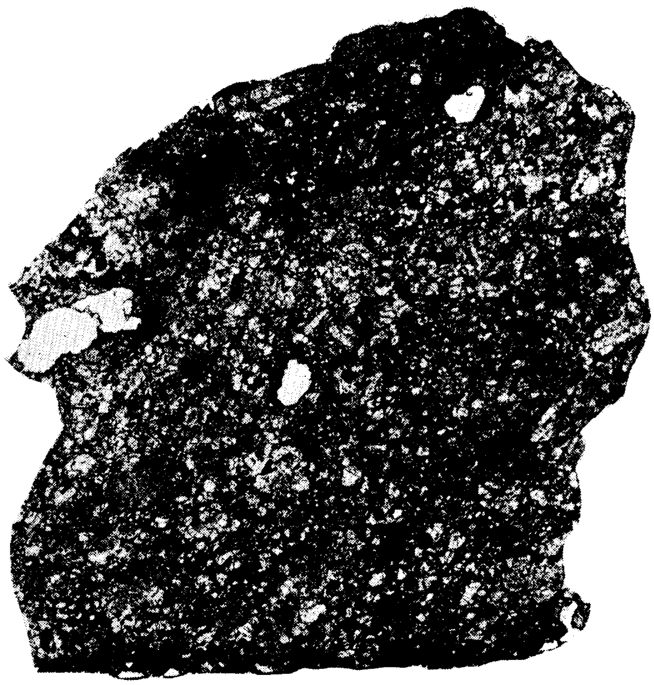

Fig. 4. Photograph of a thin section of the Yamato-75100 (type H6) chondrite showing poorly defined chondrules and recrystallized matrix. Width dimension of photograph, 8 mm.

several concentric textures (Figs. 9 and 21). Some chondrules contain glass or wholly devitrified glass or extremely fine-grained materials with a small amount of plagioclase (Figs. 9, 15 and 20). Some chondrules have glassy or recrystallized rims (Figs. 10, 23 and 26).

Porphyritic-olivine chondrules are composed mainly of medium-grained olivine

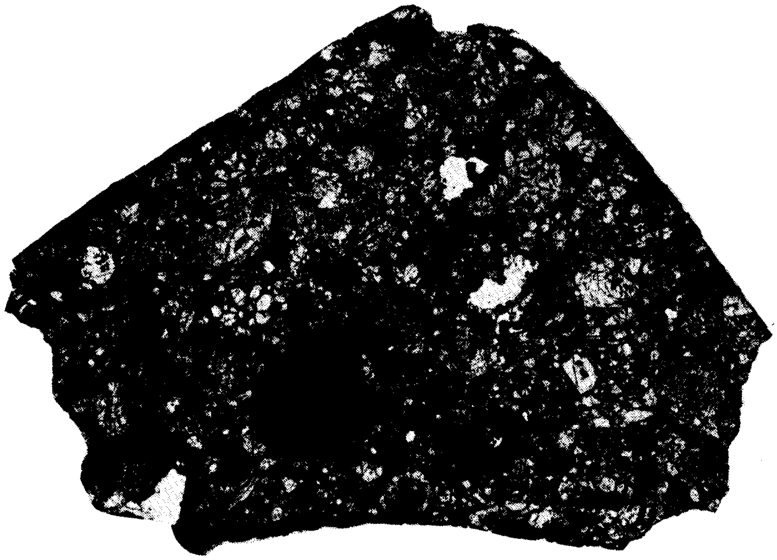

Fig. 5. Photograph of a thin section of Yamato-75019 (type L4) chondrite showing well-defined chondrules and transparent microcrystalline matrix. Long dimension of photograph, 9 mm.

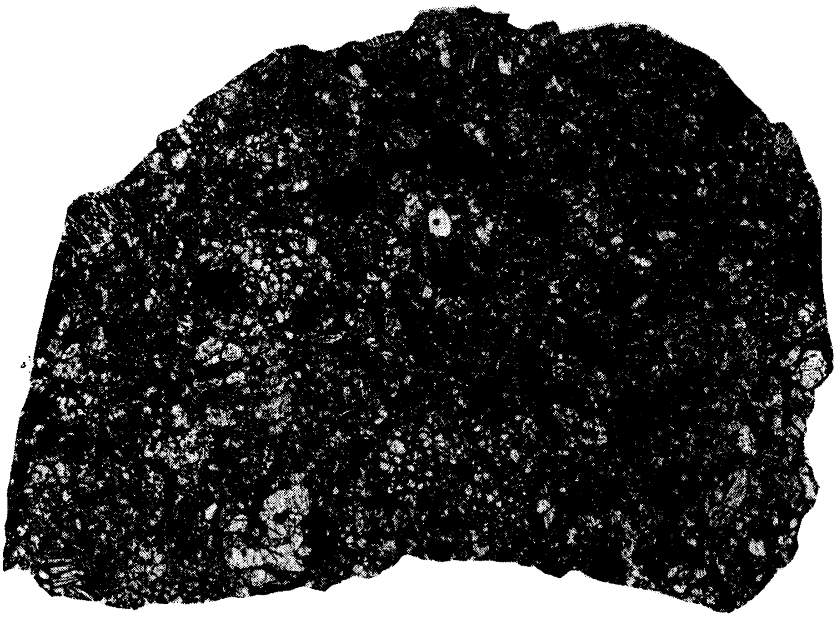

Fig. 6. Photograph of a thin section of the Yamato-75289 (type L5) chondrite showing readily delineated chondrules and recrystallized matrix. Long dimension of photograph, 13 mm.

crystals and glassy or cryptocrystalline materials (Figs. 11, 15, 19, 21 and 25). Olivine of porphyritic chondrules is rarely surrounded by narrow Ca-rich clinopyroxene rims. Porphyrititic-olivine and clinoenstatite chondrule in the Yamato-75029 chondrite consist mainly of medium-grained olivine crystals and partially of medium-grained clinoenstatite crystals ($Wo_{0.9}En_{93.7}Fs_{5.4}$–$Wo_{0.6}En_{91.9}Fs_{7.5}$) with polysynthetic twinning and glassy materials (Figs. 12 and 13). Porphyritic-olivine and orthopyroxene

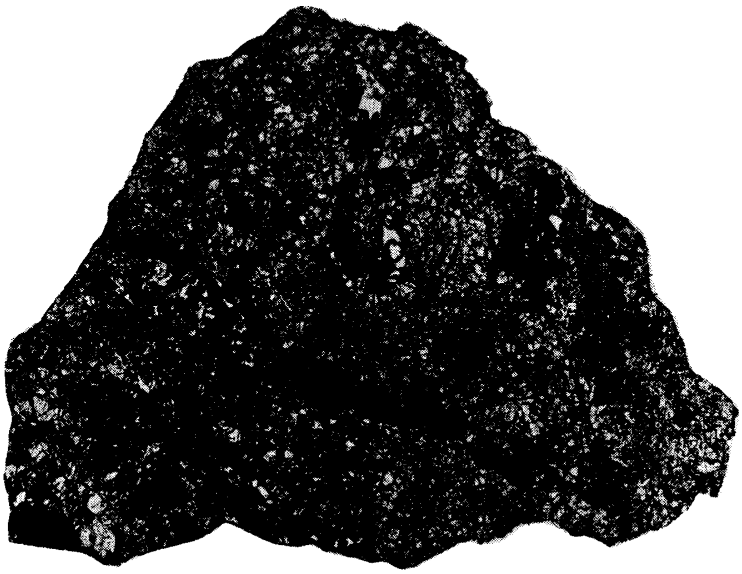

Fig. 7. Photograph of a thin section of the Yamato-75071 (type L6) chondrite showing poorly defined chondrules, recrystallized matrix and shock vein. Long dimension of photograph, 8 mm.

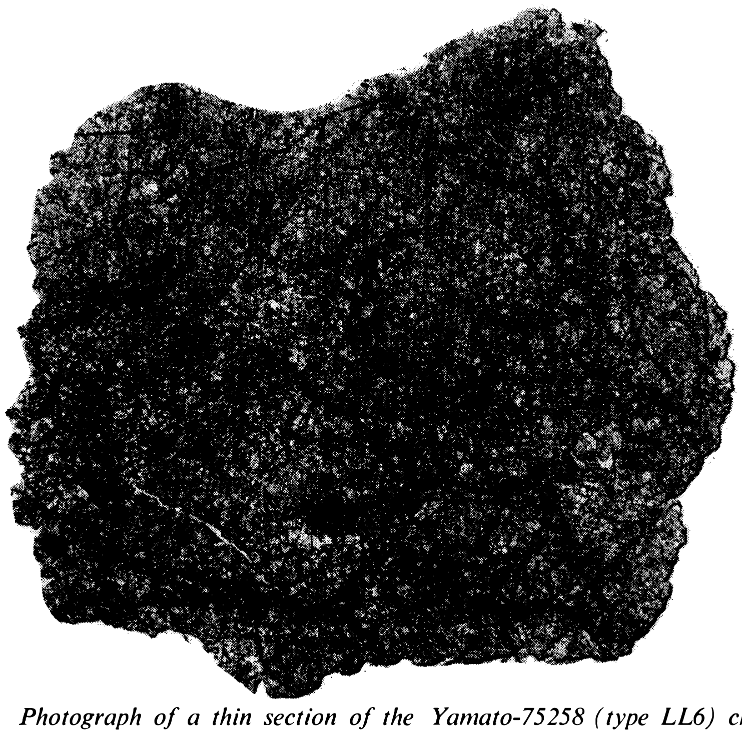

Fig. 8. Photograph of a thin section of the Yamato-75258 (type LL6) chondrite showing poorly defined chondrules and recrystallized matrix. Long dimension of photograph, 20 mm.

chondrules are composed mainly of medium-grained olivine and orthopyroxene crystals and glassy or cryptocrystalline materials (Figs. 9, 19, 20, 24 and 25). Barred-olivine chondrules are composed mainly of parallel sets of olivine crystals and glass of weakly devitrified glass (Figs. 10, 14, 16 and 17). A barred-orthopyroxene chondrule forming a herringbone pattern in the Yamato-75262 coexists with medium-grained crystals and

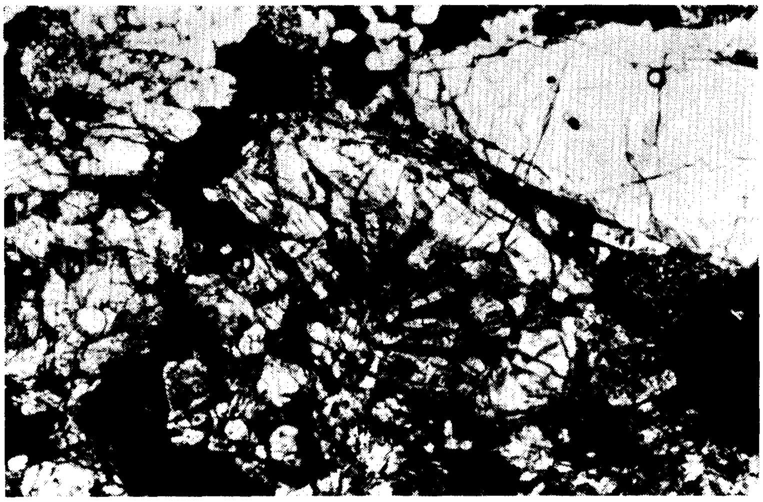

Fig. 9. Radial and porphyritic-chondrule consisting of medium-grained prismatic olivine and orthopyroxene crystals, and weakly recrystallized glass in Yamato-75012 chondrite. One nicol. Long dimension of photograph, 1.3 mm.

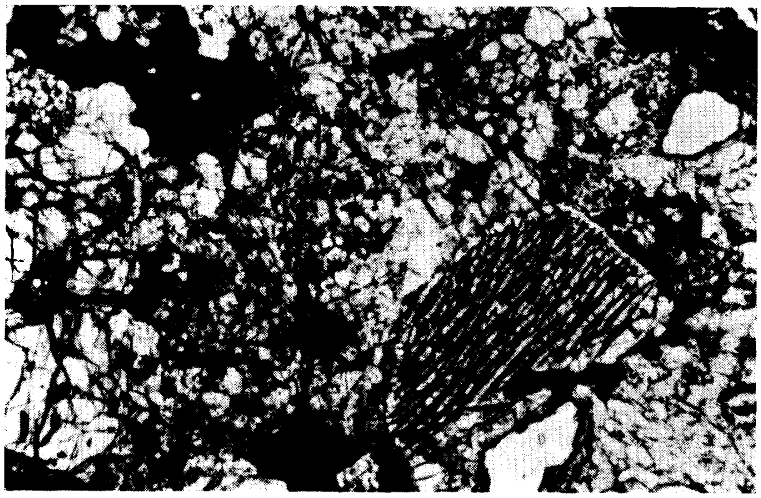

Fig. 10. Barred-olivine chondrule composed of alternate layers of olivine crystals in Yamato-75012 chondrite. The interstices between olivine bars are filled with cryptocrystalline materials and devitrified glass. One nicol. Long dimension of photograph, 1.3 mm.

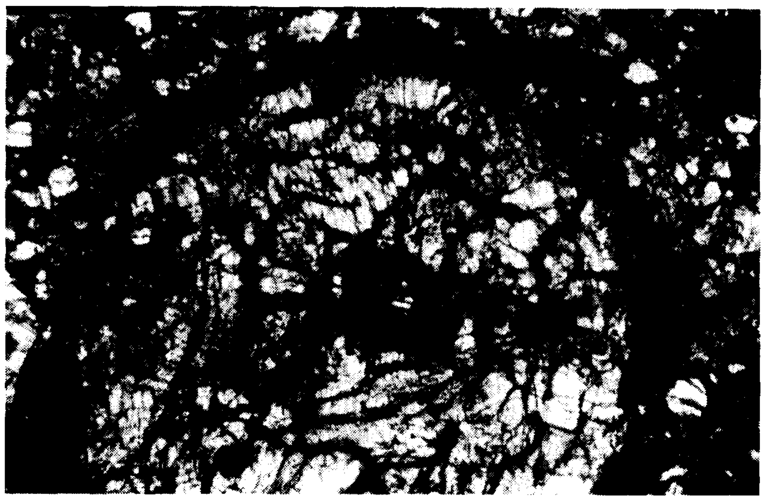

Fig. 11. Porphyritic-olivine chondrule consisting of medium-grained olivine crystals and opaque materials and glass in Yamato-75029 chondrite. One nicol. Long dimension of photograph, 1.3 mm.

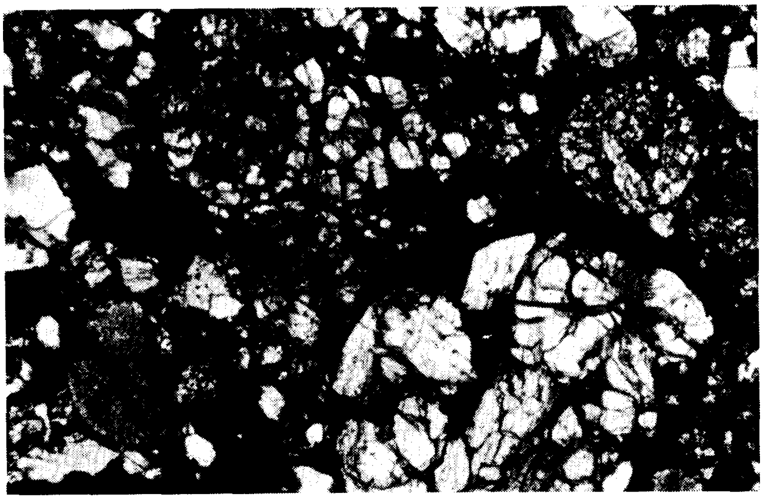

Fig. 12. A few chondrules in Yamato-75029 chondrite. A large chondrule of under part, such as porphyritic-olivine and clinoenstatite chondrule consisting of medium-grained olivine and clinoenstatite and opaque materials and glass. One nicol. Long dimension of photograph 1.3 mm.

Fig. 13. An enlarged photograph of the porphyritic-olivine and clinoenstatite chondrule of Fig. 12. A clinoenstatite crystal ($Wo_{0.9}En_{93.7}Fs_{5.4}$) with polysynthetic twinning (central part of photograph) includes fine-grained olivine crystals. Crossed nicols. Long dimension of photograph, 0.52 mm.

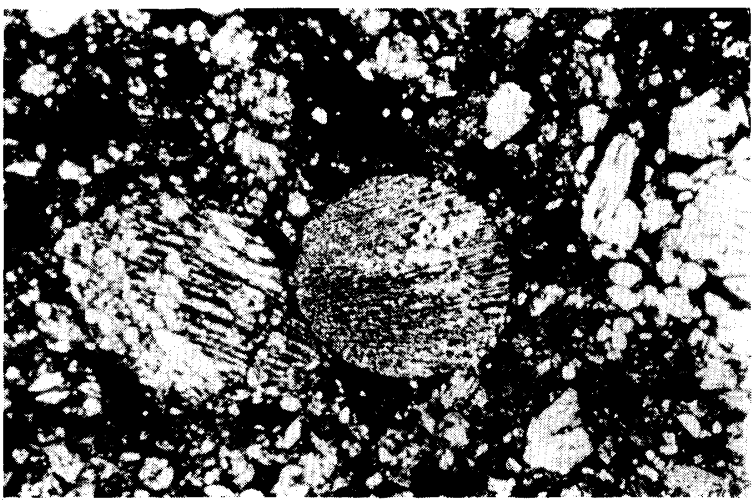

Fig. 14. Barred-olivine chondrule (left side) and radial-orthopyroxene chondrule (right side) in Yamato-75096 chondrite. The former is composed of alternate layers of olivine crystals and recrystallized material, and the latter consists of aggregate of fine prismatic orthopyroxene crystals and cryptocrystalline materials. One nicol. Long dimension of photograph, 2.6 mm.

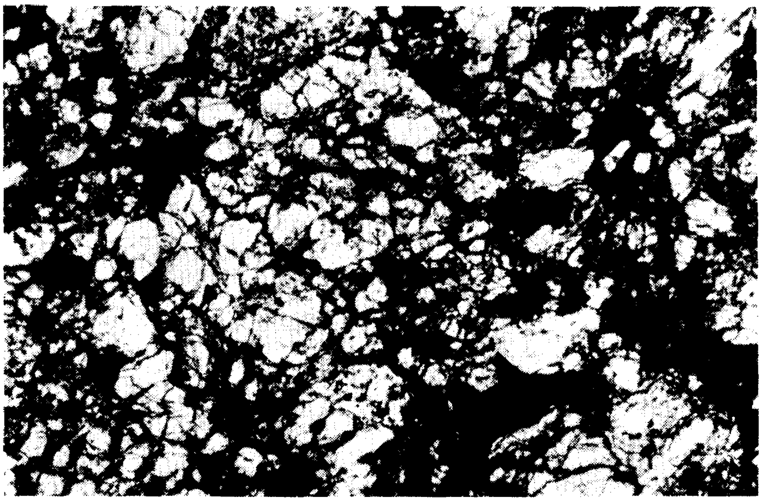

Fig. 15. Porphyritic-olivine chondrule consisting of medium-grained olivine crystals and recrystallized materials in Yamato-75100 chondrite. One nichol. Long dimension of photograph, 1.3 mm.

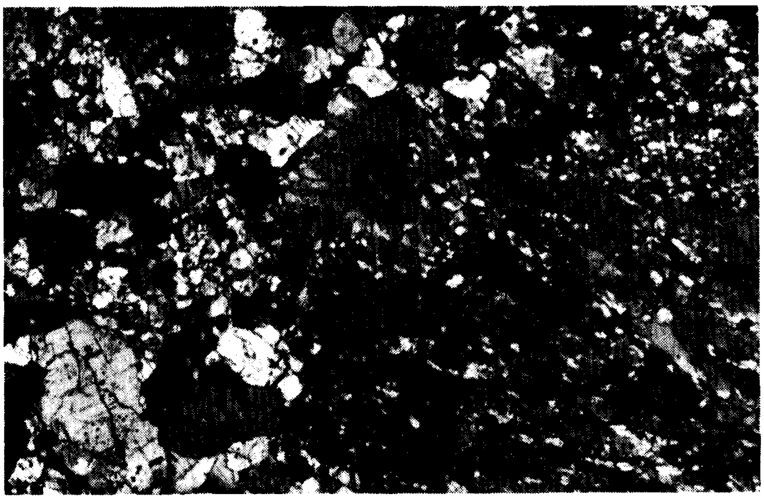

Fig. 16. A relic structure of chondrule consisting of alternate layeres of olivine and orthopyroxene crystals in Yamato-75258 chondrite. The interstices between crystal layers are filled with recrystallized materials. Crossed nicols. Long dimension of photograph, 1.3 mm.

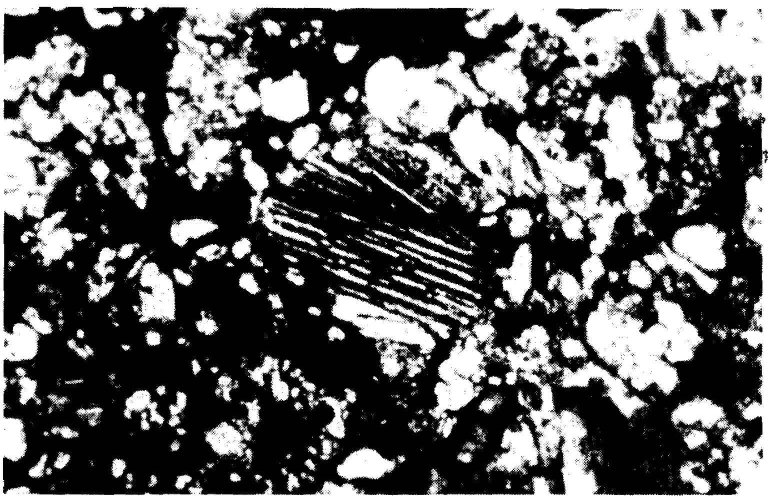

Fig. 17. Barred-olivine chondrule consisting of alternate layers of olivine crystals in Yamato-75259 chondrite. The interstices between olivine bars are filled with cryptocrystalline materials. One nicol. Long dimension of photograph, 1.3 mm.

Fig. 18. A couple of relic barred-orthopyroxene chondrules forming a herringbone pattern composed of alternate layers of orthopyroxene crystals in Yamato-75262 chondrite. The interstices between crystal layers are filled with recrystallized materials. One nicol. Long dimension of photograph, 1.3 mm.

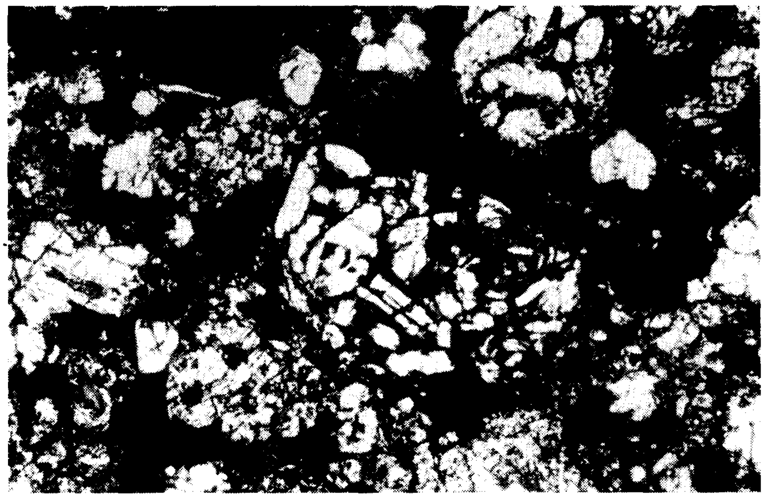

Fig. 19. Two porphyritic-olivine and orthopyroxene chondrules composed of medium-grained olivine and orthopyroxene crystals and weakly recrystallized materials in Yamato-75269 chondrite. One nicol. Long dimension of photograph, 1.3 mm.

Fig. 20. Radial-orthopyroxene (left side) and porphyritic-olivine and orthopyroxene chondrule (right side) in Yamato-75270 chondrite. The former composed of fine orthopyroxene crystals and weakly recrystallized glass, the latter consisting of olivine and orthopyroxene crystals and recrystallized materials. One nicol. Long dimension of photograph, 1.3 mm.

Fig. 21. Porphyritic-olivine chondrule with concentric feature composed of medium-grained olivine crystals and recrystallized material in Yamato-75270 chondrite. One nicol. Long dimension of photograph, 1.3 mm.

Fig. 22. Radiated barred-orthopyroxene chondrule consisting of alternate layers of fine-grained orthopyroxene crystals in Yamato-75277 chondrite. The interstices between orthopyroxene bars are filled with microcrystalline materials. One nicol. Long dimension of photograph, 1.3 mm.

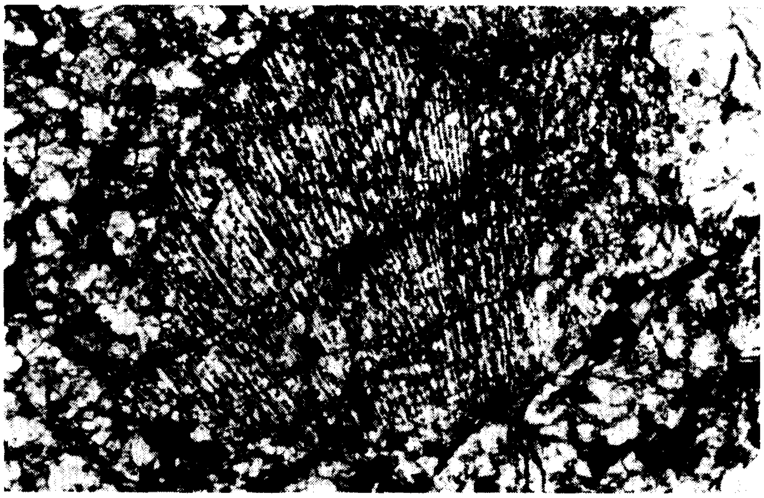

Fig. 23. Barred-orthopyroxene chondrule with radial feature composed of alternate layers of fine-grained orthopyroxene crystals in Yamato-75289 chondrite. The interstices between orthopyroxene bars are filled with cryptocrystalline materials. One nicol. Long dimension of photograph, 1.3 mm.

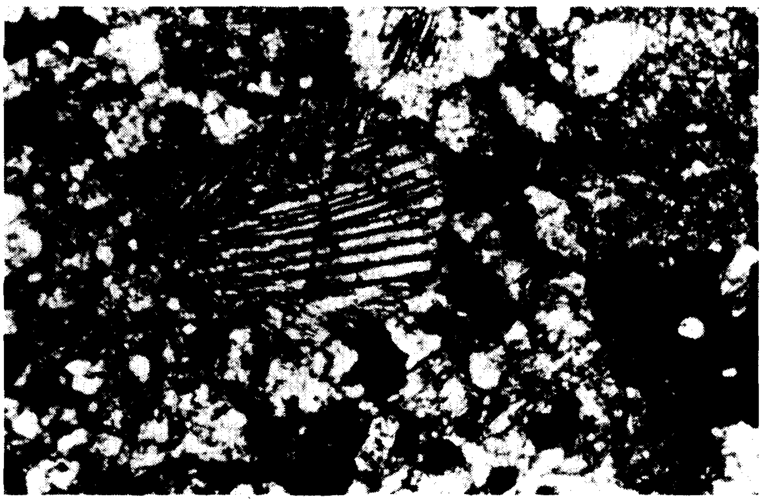

Fig. 24. A lot of chondrules in Yamato-75291 chondrite, such as porphyritic-olivine, porphyritic-olivine and orthopyroxene, and radiated porphyritic-olivine and orthopyroxene chondrules. One nicol. Long dimension of photograph, 1.3 mm.

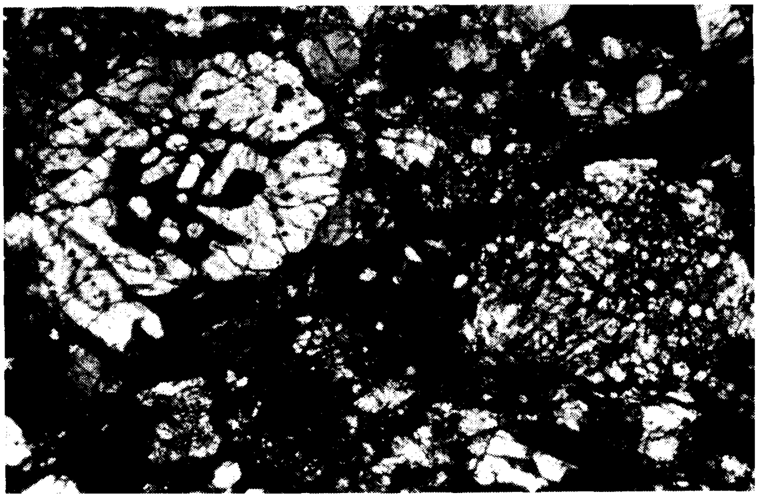

Fig. 25. Porphyritic-olivine (left side) and porphyritic-olivine and orthopyroxene (right side) chondrules in Yamato-75291 chondrite. The former consisting of medium-grained olivine crystals and weakly recrystallized glass, and the latter composed of fine-grained olivine and orthopyroxene crystals and weakly recrystallized materials. Crossed nicols. Long dimension of photograph, 1.3 mm.

Fig. 26. Radial-orthopyroxene chondrule composed of aggregate of fine prismatic orthopyroxene crystals and cryptocrystalline materials in Yamato-75291 chondrite. Crossed nicols. Long dimension of photograph, 0.52 mm.

glassy or weakly recrystallized material (Fig. 18). Radial and barred-orthopyroxene chondrules consist mainly of fine or very fine prismatic orthopyroxene crystals and glassy or cryptocrystalline materials (Figs. 19, 20, 22, 23 and 26).

Plagioclase feldspar in chondrules and matrix of petrologic types 4, 5 and 6 occurs as microcrystalline aggregates. Rarely, clear plagioclase occurs in petrologic type 6.

Table 1 shows petrologic types of the specimens determined by the textural characteristics of chondrule, matrix, plagioclase and igneous glass proposed by VAN SCHMUS and WOOD (1967) and VAN SCHMUS (1969).

4. Classification of Yamato Chondrites

Frequency distribution of iron contents (atomic %=100 Fe/(Mg+Fe)) of olivines and orthopyroxenes for the investigated samples is shown in Tables 2 and 3. The ranges of iron content (atomic %) for the average H6, L6 and LL6 chondrites are shown at the top of Tables 2 and 3 (VAN SCHMUS and WOOD, 1967; VAN SCHMUS, 1969). The mean compositions (for Mg, Fe and Ca) of olivines and orthopyroxenes, the number of measurements, the mean deviation of iron contents, and the percent mean deviations (% M.D.) of iron contents in their olivine and orthopyroxene listed in Table 4, respectively.

In Tables 2 and 3, these 19 Yamato-75 chondrites are distinctly classified as H (11 chondrites), L (7 chondrites) and LL (one chondrite) groups.

Table 4 shows that % M.D. for olivine and orthopyroxene of the Yamato-75029 chondrite has large values, such as 8.3 and 12.9. Consequently, this chondrite corresponds to the low petrologic type (unequilibrated chondrite). Six chondrites (Yamato-75096, -75262, -75269, -75291, -75019, -75297) have less than 5% M.D. for olivine and 3 to 8% M.D. for orthopyroxene. Petrologic types of these chondrites are classified as 4, 4–5 and 5–4. Twelve chondrites (Yamato-75012, -75259, -75267, -75100, -75277, -75304, -75017, -75270, -75288, -75289, -75071, -75258) have less than 3% M.D. for olivine except Yamato-75304 containing 3.4% M.D., and less than 3.3% M.D. for orthopyroxene except Yamato-75012. Generally, % M.D. for olivine and orthopyroxene of these chondrite is less than 2. Namely, these chondrites correspond to the high petrologic type (equilibrated chondrite; petrologic types 5, 5–6 and 6).

The textural characteristics of chondrule, matrix, igneous glass and secondary feldspar in these chondrites are listed in Table 1.

5. Conclusion

A preliminary classification of 19 Yamato-75 chondrites (Yamato-75012, -75017, -75019, -75029, -75071, -75096, -75100, -75258, -75259, -75262, -75267, -75269, -75270, -75277, -75288, -75289, -75291, -75297 and -75304) from East Antarctica was performed, based on the textural characteristics and electron microprobe analyses of olivine and orthopyroxene.

On the basis of the frequency distribution of iron contents of olivines and orthopyroxenes, and the microscopical characters, these chondrites are classified as H3, H4, H4–5, H5–4, H5, H5–6, H6, L4, L4–5, L5, L6 and LL6.

Table 1. Petrologic types determined by textural characteristics of several Yamato-75 chondrites.

Name	Texture of chondrule	Texture of matrix	Igneous glass	Development of feldspar	Low-Ca pyroxene	Petrologic type	Chemical group
Yamato-75012	Well-defined and readily delineated	Microcrystalline and recrystallized	Absent	Microcrystalline aggregates	opx	5	H
Yamato-75029	Very sharply defined	Opaque	Turbid glass	Absent	opx + cpx	3	H
Yamato-75096	Well-defined	Microcrystalline	Turbid glass	Microcrystalline aggregates	opx + cpx	4	H
Yamato-75100	Poorly defined	Microcrystalline and recrystallized	Absent	Microcrystalline aggregates	opx	6	H
Yamato-75259	Readily delineated	Microcrystalline and recrystallized	Absent	Microcrystalline aggregates	opx	5	H
Yamato-75262	Well-defined and readily delineated	Microcrystalline	Turbid glass	Microcrystalline aggregates, well-developed	opx	5–4	H
Yamato-75267	Poorly defined	Microcrystalline and recrystallized	Absent	Microcrystalline aggregates	opx	5–6	H
Yamato-75269	Well-defined	Transparent microcrystalline	Turbid glass	Microcrystalline aggregates and interstitial glass	opx + cpx	4	H
Yamato-75277	Poorly defined	Recrystallized	Absent	Clear, intersti-tial grains	opx	6	H
Yamato-75291	Readily delineated	Microcrystalline	Turbid glass	Microcrystalline aggregates	opx	4–5	H
Yamato-75304	Poorly defined	Recrystallized	Absent	Clear, intersti-tial grains	opx	6	H
Yamato-75017	Poorly defined and readily delineated	Recrystallized	Absent	Microcrystalline aggregates	opx	5	L
Yamato-75019	Readily delineated	Microcrystalline and recrystallized	Turbid glass	Microcrystalline aggregates	opx	4	L
Yamato-75071	Poorly defined	Recrystallized	Absent	Clear, intersti-tial grains	opx	6	L
Yamato-75270	Readily delineated	Microcrystalline and recrystallized	Turbid glass	Microcrystalline aggregates	opx	5	L
Yamato-75288	Readily delineated	Microcrystalline and recrystallized	Absent	Microcrystalline aggregates	opx	5	L

Yamato-75289	Readily delineated	Recrystallized	Absent	Microcrystalline aggregates	opx	5	L
Yamato-75297	Well-defined and readily delineated	Transparent microcrystalline	Turbid glass	Microcrystalline aggregates	opx + cpx	4–5	L
Yamato-75258	Poorly defined	Recrystallized	Absent	Clear, intersti-tial grains	opx	6	LL

Table 2. Frequency distribution of iron contents of olivines.

Sample	Atomic % Fe 11	12	13	14	15	16	17	18	19	20	21	22	23	24	25	26	27	28	29	30	31	32	35
						———	———	H	———	———		———	L	———	———		———	———	LL	———	———		
Y-75012								+	++	+													
Y-75029	–					–	+	+	+	–	–												
Y-75096					–	+	++																
Y-75100								++	+	–													
Y-75259								–	++	+													
Y-75262						+	++	+	–	–													
Y-75267						+	++	+	–	–													
Y-75269							++	+															
Y-75277							+	++															
Y-75291					–	++	+	+	–	–				–									
Y-75304						+	++	+			–												
Y-75017												–	++										
Y-75019												+	++	+									
Y-75071													+	++	–								
Y-75270													–	++	+								
Y-75288												–	++	+									
Y-75289													++	+			–						
Y-75297											–	++	++	–									
Y-75258																		–	++	++	–	–	

–: 10%>, +: 10–40%, ++: 40%<.

Table 3. Frequency distribution of iron contents of low-Ca pyroxenes.

	Atomic % Fe																					
Sample	5	6	7	8	9	10	11	12	13	14	15	16	17	18	19	20	21	22	23	24	25	26
											——H——				——L——				——LL——			
Y-75012												++			+							
Y-75029	–		–						–		+	++	–	–		–						
Y-75096						–	–			–	++	+	–								–	
Y-75100											+	++	–									
Y-75259												++	++									
Y-75262											+	++	–	–	–							
Y-75267											++	+	+									
Y-75269								–	–		++	+			–							
Y-75277												++	+	–								
Y-75291									+		+	++	+									
Y-75304											+	++	+	–								
Y-75017														+	+	++	+					
Y-75019															+	++						
Y-75071																++	+					
Y-75270																–	++	+	+			
Y-75288															–	++	+					
Y-75289																++	+					
Y-75297													+		+	++	+		+			
Y-75258																			++	++		

–: 10%>, +: 10–40%, ++: 40%<.

Table 4. Mean composition and percent mean deviation (% M.D.) of olivines and low-Ca pyroxenes.

Name	Olivine					Pyroxene						
	No.	Mg	Fe	M.D.	%M.D.	No.	Ca	Mg	Fe	M.D.	%M.D.	Remarks
Y-75012	27	80.7	19.3	0.43	2.2	8	1.1	81.7	17.2	1.10	6.5	H5
Y-75029	29	81.6	18.4	1.53	8.3	28	1.3	82.2	16.5	2.12	12.9	H3
Y-75096	27	82.8	17.2	0.35	2.0	23	1.2	82.9	15.9	0.26	7.9	H4
Y-75100	21	81.2	18.8	0.41	2.2	14	1.5	82.1	16.4	0.28	1.7	H6
Y-75259	24	80.2	19.8	0.31	1.6	22	1.5	81.4	17.1	0.25	1.5	H5
Y-75262	26	81.2	18.8	0.70	3.7	21	1.4	81.9	16.7	0.76	4.5	H5–4
Y-75267	24	81.3	18.7	0.56	3.0	13	1.4	82.4	16.2	0.45	2.8	H5–6
Y-75269	33	81.3	18.7	0.25	1.3	27	0.6	83.6	15.8	0.64	4.1	H4
Y-75277	31	80.8	19.2	0.31	1.6	16	1.4	81.8	16.8	0.36	2.2	H6
Y-75291	58	81.5	18.5	0.89	4.8	10	0.9	83.0	16.1	0.55	3.4	H4–5
Y-75304	57	81.5	18.5	0.63	3.4	20	1.3	82.4	16.3	0.54	3.3	H6
Y-75017	25	75.5	24.5	0.20	0.8	9	1.0	78.7	20.3	0.62	3.1	L5
Y-75019	63	75.7	24.2	0.42	1.7	13	1.3	78.4	20.3	0.63	3.1	L4
Y-75071	22	74.7	25.3	0.39	1.5	7	1.5	77.7	20.8	0.36	1.7	L6
Y-75270	32	74.2	25.7	0.40	1.5	19	1.2	77.0	21.9	0.57	2.6	L5
Y-75288	26	75.2	24.8	0.38	1.5	12	1.4	77.8	20.8	0.33	1.6	L5
Y-75289	40	75.0	25.0	0.45	1.8	10	1.4	77.7	20.9	0.45	2.2	L5
Y-75297	49	75.9	24.0	0.38	1.6	10	1.3	78.2	20.6	0.96	4.7	L4–5
Y-75258	46	68.1	31.2	0.53	1.7	10	2.3	73.6	24.1	0.26	1.1	LL6

Acknowledgments

The authors wish to express their gratitude to Prof. T. Hoshiai of the National Institute of Polar Research, for his kind suggestions and valuable advice for the survey by the JARE-16 Yamato party. The authors are indebted to the members of the Yamato party for their help in collecting the meteorites. We thank Dr. K. Yanai and Mr. G. Azuma of the National Institute of Polar Research for their help in preparing the thin sections.

References

Albee, A. L. and Ray, L. (1970): Correction factors for electron probe microanalysis of silicates, oxides, carbonates, and sulfates. Anal. Chem., **42**, 1408–1414.

Bence, A. E. and Albee, A. L. (1968): Empirical correction factors for the electron microanalysis of silicates and oxides. J. Geol., **76**, 382–403.

Dodd, T. R., Jr., Van Schmus, W. R. and Koffmann, D. M. (1967): A survey of the unequilibrated ordinary chondrites. Geochim. Cosmochim. Acta, **31**, 921–951.

Matsumoto, Y. (1978): Collection of Yamato meteorites, East Antarctica in November and December 1975, and January 1976. Mem. Natl Inst. Polar Res., Spec. Issue, **8**, 38–50.

Matsumoto, Y. and Hayashi, M. (1980): A classification of several Yamato-75 chondrites. Mem. Natl Inst. Polar Res., Spec. Issue, **17**, 21–31.

Matsumoto, Y., Hayashi, M., Miyamoto, M., Takeda, H. and Yanai, K. (1979): A classification of the Yamato-75 chondrites based on chemical compositions of olivines and pyroxenes. Mem. Natl Inst. Polar Res., Spec. Issue, **12**, 72–81.

Matsumoto, Y., Hayashi, M., Daishi, M. and Miúra, Y. (1981): On homogeneity of the Yamato-75110 chondrite. Mem. Natl Inst. Polar Res., Spec. Issue, **20**, 106–118.

Miúra, Y. and Matsumoto, Y. (1981): Classification of several Yamato-75 chondrites (III). Mem. Natl Inst. Polar Res., Spec. Issue, **20**, 53–68.

MIÚRA, Y. and MATSUMOTO, Y. (1982): Classification of several Yamato-75 chondrites (IV). Mem. Natl Inst. Polar Res., Spec. Issue, **25**, 1–16.

VAN SCHMUS, W. R. (1969): The mineralogy and petrology of chondritic meteorites. Earth Sci. Rev., **5**, 145–184.

VAN SCHMUS, W. R. and WOOD, J. R. (1967): A chemical-petrologic classification for the chondritic meteorites. Geochim. Cosmochim. Acta, **31**, 747–765.

YANAI, K., MIYAMOTO, M. and TAKEDA, H. (1978): A classification for the Yamato-74 chondrites based on the chemical compositions of their olivines and pyroxenes. Mem. Natl Inst. Polar Res., Spec. Issue, **8**, 110–120.

(Received July 16, 1984; Revised manuscript received December 1, 1984)